Hydrogen motion and local structure of metals in β-$Ti_{1-y}V_yH_x$ as studied by ^1H NMR

Takahiro Ueda, Shigenobu Hayashi, and Kikuko Hayamizu
National Chemical Laboratory for Industry, Tsukuba, Ibaraki 305, Japan
(Received 23 June 1992; revised manuscript received 26 February 1993)

Hydrogen motion in β-$Ti_{1-y}V_yH_x$ ($y=0.2$, 0.4, 0.6, and 0.8; $x\sim1$) alloys was studied by ^1H NMR, with which the temperature and frequency dependences of proton spin-lattice relaxation times (T_1) were measured over the temperature range 105–400 K and at frequencies 9, 22.5, 52, and 90 MHz. The temperature dependences of T_1 change systematically with the metal composition; with a decrease in the concentration of V, the minimum value of T_1 increases and the temperature at which T_1 is minimized shifts to the higher-temperature side. These results are analyzed with two-site jumps of a proton between unequal potential wells, in which Brouwer's model is assumed to describe local structure of the alloys. Good agreement between the experimental and calculated T_1 values is given by this treatment, unlike the isotropic diffusion model. The following three parameters are used for the calculation: activation energies for Ti and V are $E_{Ti}=16$ and $E_V=9.5$ kJ/mol, respectively, and the frequency prefactor is $\tau_0=1.5\times10^{-11}$ s for $0.4\le y\le0.8$. The obtained E_{Ti} and E_V values agree with those of pure metal hydrides such as TiH_x and VH_x, respectively.

INTRODUCTION

Titanium and vanadium metals form a solid solution with a body-centered-cubic (bcc) structure over wide ranges of composition and temperature.[1] The Ti-V alloys form stable hydrides,[2,3] which are expected to have continuously varying properties depending on their composition. The Ti-V alloys absorb hydrogen until the ratio of hydrogen-to-metal atoms reaches two. This dihydride phase, called γ-Ti-V-H, has a face-centered-cubic (fcc) lattice at room temperature.[4] The arrangement of hydrogen atoms and several properties, such as electronic structure[5–7] and phase separation,[4,8] has been studied extensively by means of ^1H and ^{51}V NMR. Previously we have found that when the Ti-V alloys are hydrogenated under several high pressures of hydrogen gas, the given hydrides are separated into three or even four phases in most cases.[4,9,10] We have characterized the Ti-V-H system by means of ^1H and ^{51}V NMR and powder x-ray diffraction,[7] and found that the Ti-V-H system separates into α-Ti-V-H, β-Ti-V-H, γ-Ti-V-H, and γ-TiH_x. However, we have succeeded in synthesizing hydride samples composed of only the β-Ti-V-H phase, and found that the host metals form a simple bcc lattice.[8,11] If the hydrogen motion in the β phase is clearly understood, one can expect to define the arrangement of Ti and V atoms around a hydrogen atom and the potential wells for the interaction between each metal and the hydrogen atom. We have studied hydrogen motion in the β phase through spin-lattice relaxation times by means of ^1H NMR, but the hydrogen motion was difficult to explain using the mechanism of the simple isotropic diffusion.[10]

In this work, we have reinvestigated the hydrogen motion in the β phase by observing temperature and frequency dependences of proton spin-lattice relaxation times (T_1). To improve the agreement between the experimental and calculated T_1, we try to analyze the results using a two-site jump model combined with unequal potential wells and taking into consideration local structures of metal atoms around a hydrogen atom. The local structure around a hydrogen atom is assumed to be statistically determined by the composition of the metal atoms. This treatment gives a more qualitative agreement between the experimental data and the calculated values without adjustment of the coefficient than the isotropic diffusion model does.

EXPERIMENTAL

Three of the Ti-V monohydride (β-Ti-V-H) samples studied were the same as those used in Ref. 11: $Ti_{0.2}V_{0.8}H_{0.83}$, $Ti_{0.4}V_{0.6}H_{0.91}$, and $Ti_{0.6}V_{0.4}H_{0.91}$. These three samples had been confirmed to consist of only the β-Ti-V-H phase.[11] $Ti_{0.8}V_{0.2}H_{1.98}$ was synthesized by reac-

TABLE I. The lattice constants for each metal hydride and the interhydrogen distances for the first-, second-, third-, and fourth-nearest neighbor sites.

Metal hydride	a_0/nm	First	Second	Third	Fourth
$Ti_{0.2}V_{0.8}H_{0.83}$	0.3208[a]	0.1134	0.1604	0.1964	0.2268
$Ti_{0.4}V_{0.6}H_{0.91}$	0.3263[a]	0.1154	0.1632	0.1998	0.2307
$Ti_{0.6}V_{0.4}H_{0.91}$	0.3300[a]	0.1667	0.1650	0.2021	0.2333
$Ti_{0.8}V_{0.2}H_{0.89}$	0.3334	0.1179	0.1667	0.2041	0.2357

[a]Reference 11.

tion between a Ti-V alloy ($Ti_{0.8}V_{0.2}$) and hydrogen gas under the H_2 pressure less than 1 atom at 700 °C. $Ti_{0.8}V_{0.2}H_{0.89}$ was obtained by dehydrogenation of the dihydride under a reduced pressure at 300~400 °C. These specimens were sealed off in ampoules under vacuum.

The instrument used for the ^1H T_1 measurements was a Bruker CXP 100 pulsed spectrometer. The T_1 values were measured in the temperature range between 105–400 K, and at four frequencies, 9, 22.5, 52, and 90 MHz. They were measured by the 90°-τ-90° method, and the error was less than ±5%. The temperature of the samples was controlled by the flow of cooled or heated nitrogen gas with the accuracy of ±1 K.

Powder x-ray-diffraction patterns for the metal hydrides were measured by a Rigaku Geiger-flex diffractometer with Cu $K\alpha$ irradiation at room temperature. The lattice constants obtained are listed in Table I, and were used in the theoretical calculations of the ^1H T_1.

RESULTS

The magnetization recovery curves for $Ti_{0.2}V_{0.8}H_{0.83}$, $Ti_{0.4}V_{0.6}H_{0.91}$, and $Ti_{0.6}V_{0.4}H_{0.91}$ were described by a single exponential decay over all temperatures, but for $Ti_{0.8}V_{0.2}H_{0.89}$ nonexponential decays over all temperature ranges were shown. The samples, except for $Ti_{0.8}V_{0.2}H_{0.89}$, consist of only the β phase, as reported previously.[11] On the other hand, $Ti_{0.8}V_{0.2}H_{0.89}$ was found to consist of four phases, being confirmed by means of ^1H magic-angle-spinning NMR spectra.[12] This phase separation is considered to be caused by the preparation procedure including repeated hydrogenations, and thus it is not an intrinsic phenomenon. Consequently, the dynamics of protons in the β phase is derived from the T_1 values observed for $Ti_{0.2}V_{0.8}H_{0.83}$, $Ti_{0.4}V_{0.6}H_{0.91}$, and $Ti_{0.6}V_{0.4}H_{0.91}$.

The ^1H T_1 values of the four samples are plotted as a function of inverse temperature in Fig. 1. The apparent T_1 values for $Ti_{0.8}V_{0.2}H_{0.89}$ are shown only for reference,

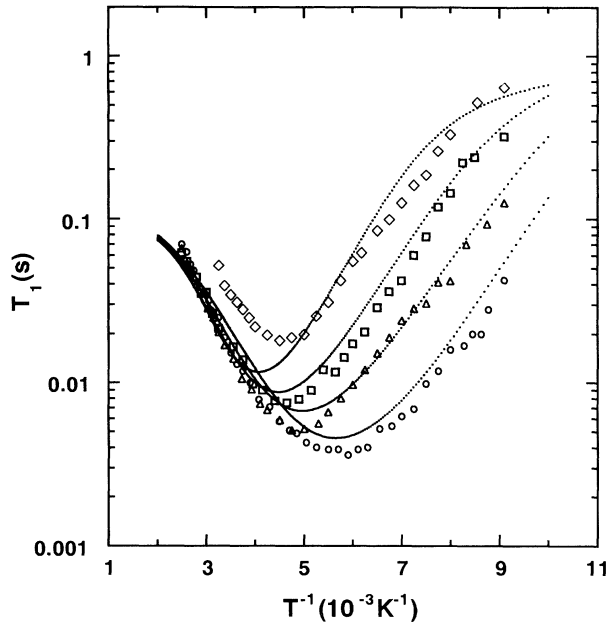

FIG. 1. Composition dependence of proton spin-lattice relaxation times (T_1) at 9 MHz; $Ti_{0.2}V_{0.8}H_{0.83}$ (○), $Ti_{0.4}V_{0.6}H_{0.91}$ (△), $Ti_{0.6}V_{0.4}H_{0.91}$ (□), and $Ti_{0.8}V_{0.2}H_{0.89}$ (◇). Solid lines are the results of calculation with our model, using $E_{Ti}=16$ kJ/mol, $E_V=9.5$ kJ/mol, and $\tau_0=1.5\times10^{-11}$ s. The contribution of conduction electrons is taken into consideration.

which were estimated from a linear part of the recovery curves. It is clearly shown that the ^1H T_1 depends on the composition of the Ti-V alloys. As the fraction of titanium in the alloys increases, the minimum of T_1 shifts to the higher-temperature side. The temperatures at which the T_1 minimum is observed are 174, 200, 215, and 217 K for $Ti_{0.2}V_{0.8}H_{0.83}$, $Ti_{0.4}V_{0.6}H_{0.91}$, $Ti_{0.6}V_{0.4}H_{0.91}$, and $Ti_{0.8}V_{0.2}H_{0.89}$, respectively. The T_1 minimum values are larger for the alloys having the lower concentrations of V: they are 3.8, 5.2, 7.5, and 18 ms for $Ti_{0.2}V_{0.8}H_{0.83}$,

TABLE II. The activation parameters and Korringa constants for each metal hydride.

Metal hydride	E_a[a] (kJ mol^{-1}) HTR[b]	LTR[c]	τ_0 (10^{-11} s)	E_{Ti} (kJ mol^{-1})	E_V (kJ mol^{-1})	K (s K)
$TiH_{0.70}$				14.2[d]		55±5[d]
$VH_{0.77}$					10~24[e]	102[f]
$V_{0.9}Cr_{0.1}H_{0.65}$					9.7[g]	
$Ti_{0.2}V_{0.8}H_{0.83}$	12.4	6.7				93
$Ti_{0.4}V_{0.6}H_{0.91}$	12.5	6.9	1.5±0.5	16±1	9.5±1	83
$Ti_{0.6}V_{0.4}H_{0.91}$	10.5	8.8				74
$Ti_{0.8}V_{0.2}H_{0.89}$	7.7	9.1				69[h]

[a]The apparent activation energy at 9 MHz.
[b]High-temperature range.
[c]Low-temperature range.
[d]Reference 32.
[e]Reference 10.
[f]Reference 33.
[g]Reference 37.
[h]This value is determined experimentally from the relaxation rate measured at 90 MHz.

$Ti_{0.4}V_{0.6}H_{0.91}$, $Ti_{0.6}V_{0.4}H_{0.91}$, and $Ti_{0.8}V_{0.2}H_{0.89}$, respectively. In the high-temperature range ($\omega_0\tau \ll 1$), the T_1 values of the different samples agree with each other except for $Ti_{0.8}V_{0.2}H_{0.89}$. On the other hand, in the low-temperature range ($\omega_0\tau \gg 1$) the T_1 values increase proportionally to the concentration of Ti. The apparent activation energies for the hydrogen motion do not show any clear composition dependences, as listed in Table II. However, the curvature in the T_1 vs $1/T$ plot around the T_1 minimum depends on the composition. As the fraction of Ti increases, the radius of the curvature in the T_1 vs $1/T$ plot becomes short, as shown in Fig. 1.

Frequency dependences of T_1 have been measured for all the samples at the four frequencies. Figures 2(a), 2(b), and 2(c) show the results for $Ti_{0.2}V_{0.8}H_{0.83}$, $Ti_{0.4}V_{0.6}H_{0.91}$, and $Ti_{0.6}V_{0.4}H_{0.91}$, respectively. For example, in Fig.

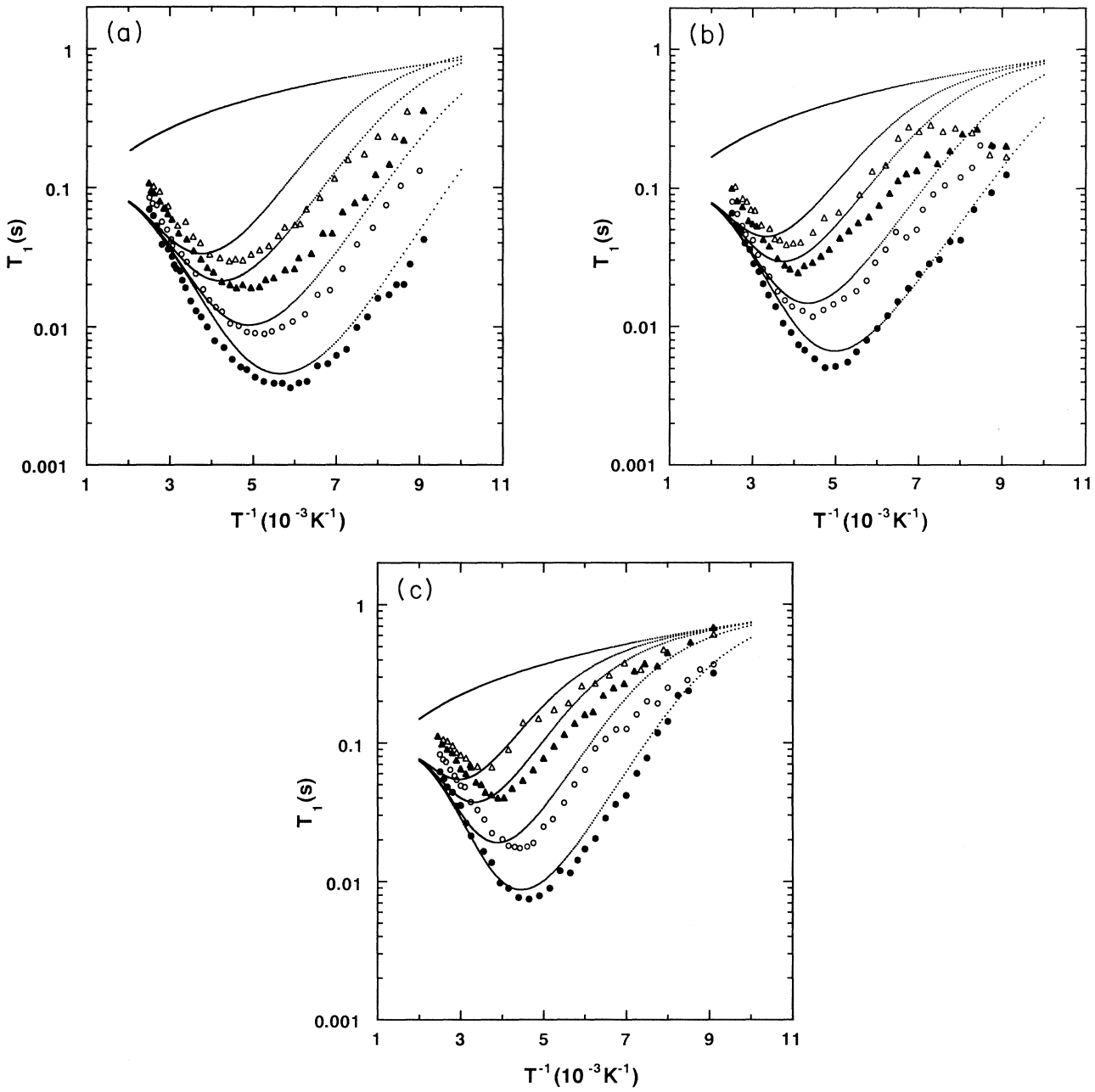

FIG. 2. Temperature and frequency dependences of proton spin-lattice relaxation times (T_1) for $Ti_{0.2}V_{0.8}H_{0.83}$ (a), $Ti_{0.4}V_{0.6}H_{0.91}$ (b), and $Ti_{0.6}V_{0.4}H_{0.91}$ (c). The resonance frequencies are 9 MHz (●), 22.5 MHz (○), 52 MHz (▲), and 90 MHz (△). Solid lines are the results of calculation with our model, using $E_{Ti}=16$ kJ/mol, $E_V=9.5$ kJ/mol, and $\tau_0=1.5\times10^{-11}$ s. The top line shows the contribution of conduction electrons, in which the Korringa constant $K(=T_{1e}\cdot T)$ is assumed to be the weighted average of the K's for TiH_x and VH_x.

2(a), the T_1 minimum observed at 9 MHz is about 200 K and shifts to the higher-temperature side as the frequency increases. The T_1 values are dependent on the frequency not only in the low- but also in the high-temperature ranges. For example, the T_1 values at 364 K were 40, 53, 73, and 85 ms at 9, 22.5, 52, and 90 MHz, respectively. The other two samples exhibit similar behavior as shown in Figs. 2(b) and 2(c), except for $Ti_{0.8}V_{0.2}H_{0.89}$. This behavior is different from the frequency dependence in the simple isotropic diffusion model.[13]

DISCUSSION

We assume that fluctuations of the dipolar interactions due to hydrogen motion in the Ti-V-H system are a dominant mechanism of T_1 in the temperature range studied, because the T_1 minimum exists and the apparent activation energies are relatively large. In addition, we cannot neglect the contribution from conduction electrons. Experimentally, there are three characteristics in the composition dependence of the T_1 values: The first is that the minimum values of T_1 increase with the fraction of Ti in the alloys. The ^{51}V-^{1}H dipolar interaction is one of the dominant mechanisms in the ^{1}H T_1. Therefore, when the fraction of vanadium decreases, the value of the T_1 minimum increases. The second is the shift of the temperature of the T_1 minimum to the higher-temperature side with increase in the Ti concentration. This means that with the increase in the Ti concentration, the hydrogen diffusion becomes slow. The potential depth for the sites surrounded by Ti is considered to be deeper than that for the sites surrounded by V. The activation energies for the hydrogen motion would reflect the affinity of hydrogen atoms with surrounding metals. For example, the activation energy for TiH_x is larger than that for VH_x. That is, the affinity of hydrogen atoms with Ti are larger than that with V. This trend has been explained by the electronegativities of metals whose order is Ti < V.[14] This work suggests that the above affinity is valid even in the Ti-V alloys. At this point the electronegativities might depend on the number of the 3*d* electrons of V, which has an excess electron compared to Ti.[15,16] The molecular orbital calculation is needed to confirm the above assumption.

The temperature and frequency dependences of the T_1 obtained in this work cannot be explained by the simple isotropic diffusion model in the following four aspects: (1) The calculated values of the T_1 minimum are much smaller than the experimental ones. (2) The slopes of the T_1 curves are asymmetric on both sides of the T_1 minimum. (3) The frequency dependence of T_1 is observed at the high-temperature side of the T_1 minimum. (4) The radius of the curvature in the T_1 vs $1/T$ plot becomes short as the fraction of Ti increases.

In the simple isotropic diffusion model, the varieties in the local structures around hydrogen atoms are neglected and all the hydrogen atoms are assumed to have the same correlation time for the diffusion. To solve these problems, we take into consideration the local structures around the hydrogen atoms. We propose a method in which the two-site jump model in the unequal potential well is combined with Brouwer's local-structure model.

In recent years hydrogens in amorphous metals and crystalline alloys have been studied theoretically[17,18] and experimentally.[19–22] In general, hydrogen atoms in alloys or metals with a bcc lattice locate at tetrahedral sites, being coordinate by four nearest-neighbor metal atoms.[23–25] Brouwer and co-workers have proposed a model for interstitial hydrogen diffusion in disordered alloys such as $Nb_{1-y}V_y$ (Ref. 17) and $Ti_{1-y}V_y$ (Ref. 18). In $Ti_{1-y}V_yH_x$ with bcc lattice, they have assumed that there are five kinds of arrangements of the two metals around one hydrogen, as shown in Fig. 3, in which $H(Ti_{4-i}V_i)$ represents a hydrogen site surrounded by $4-i$ titanium and i vanadium atoms. The populations of $H(Ti_{4-i}V_i)$ depend on the fraction of vanadium, y. The five sites have different potential energies for the hydrogen atoms. In addition, they assumed that Ti clustering takes place in the Ti-V alloys, and applied the model to the low concentration regions of hydrogen, ca. x (hydrogen-to-metal ratio) ≤ 0.1. They succeeded in their description of the diffusion in terms of single-jump processes with an activation energy and a prefactor depending on the chemical and physical structures of the initial and final sites.

The local structure is expected to be important in this system because it is one of the factors defining the state of a hydrogen atom. We introduce Brouwer's model to describe the local structure around a hydrogen atom under an assumption for simplification. The assumption is that Ti and V atoms are distributed quite randomly and homogeneously, that is, no clustering of Ti takes place in the alloys. The populations of the five sites are determined statistically by the metal compositions of the alloys. We expand Brouwer's model to the higher hydrogen concentration regions, $x \sim 1$, where the hydrogen motion has not yet been reported experimentally or theoretically. Hereafter, we call this model "Brouwer's local-structure model."

On the other hand, several research groups[26–30] have proposed that the T_1 of proton can be described by a

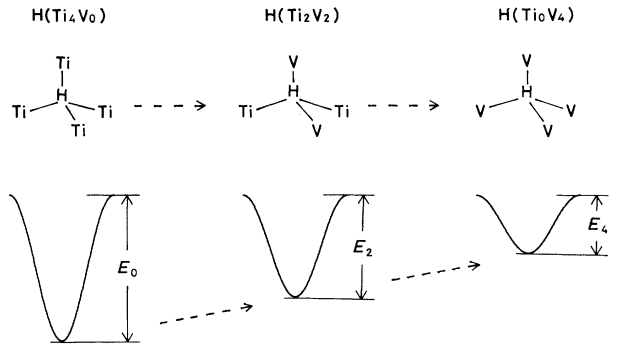

FIG. 3. Arrangements of metal atoms around a hydrogen atom, and their potential wells. E_i is the potential depth of a hydrogen atom surrounded by $4-i$ titanium atoms and i vanadium atoms. The potential depth becomes more shallow proportionally with increase of the number of the vanadium atoms.

two-site jump model in unequal potential wells. They applied the model to molecular reorientation in hydrocarbons,[28] and to jump motion of a proton forming a hydrogen bond.[29,30] Expanding the two-site jump model in unequal potential wells to Brouwer's local-structure model we analyze the experimental results.

At first, we introduce general formulas of T_1 for protons jumping between unequal potential wells in the Ti-V-H system. The total spin-lattice relaxation times in the β-Ti-V-H system are described by three components as follows:

$$T_1^{-1}=T_{1(\mathrm{VH})}^{-1}+T_{1(\mathrm{HH})}^{-1}+T_{1e}^{-1}\ , \tag{1}$$

where $T_{1(\mathrm{VH})}^{-1}$ is a contribution of the ^{51}V-^{1}H dipolar interaction, $T_{1(\mathrm{HH})}^{-1}$ that of the ^{1}H-^{1}H dipolar interaction, and T_{1e}^{-1} that of the interaction with conduction electrons, which satisfies the Korringa relation $[T_{1e}\cdot T=K(\mathrm{const})]$. Contributions of the ^{47}Ti-^{1}H and ^{49}Ti-^{1}H dipolar interactions to the total T_1 are negligible because of low natural abundances and small gyromagnetic ratios of both ^{47}Ti and ^{49}Ti, although ^{47}Ti and ^{49}Ti have a nuclear spin, $I=\frac{5}{2}$ and $\frac{7}{2}$, respectively.

$T_{1(\mathrm{VH})}$ and $T_{1(\mathrm{HH})}$ can be written as Eqs. (2) and (3) by using the two-site jump model in the unequal potential wells for the cases of unlike-spin and like-spin, following Takeda and co-workers[28–30] and Look and Lowe,[26] respectively:

$$\begin{aligned}T_{1(\mathrm{VH})}^{-1}=&\tfrac{2}{15}\gamma_{\mathrm{V}}^2\gamma_{\mathrm{H}}^2\hbar^2S(S+1)F_{\mathrm{VH}}C_{\mathrm{V}}\\&\times[J(2\tau,\omega_{\mathrm{H}}-\omega_{\mathrm{V}})+3J(2\tau,\omega_{\mathrm{H}})\\&+6J(2\tau,\omega_{\mathrm{H}}+\omega_{\mathrm{V}})]\ ,\end{aligned} \tag{2}$$

and

$$\begin{aligned}T_{1(\mathrm{HH})}^{-1}=&\tfrac{2}{5}\gamma_{\mathrm{H}}^4\hbar^2I(I+1)F_{\mathrm{HH}}C_{\mathrm{H}}\\&\times[J(\tau,\omega_{\mathrm{H}})+4J(\tau,2\omega_{\mathrm{H}})]\ ,\end{aligned} \tag{3}$$

where γ_{V} and γ_{H} are gyromagnetic ratios, ω_{V} and ω_{H} are Zeeman frequencies, and S and I are nuclear magnetic quantum numbers for ^{51}V and ^{1}H, respectively, ($S=\frac{7}{2}$ and $I=\frac{1}{2}$). $\hbar$ is Planck's constant. C_{V} and C_{H} are concentrations of vanadium and hydrogen, respectively, $C_{\mathrm{V}}=y/6$ and $C_{\mathrm{H}}=x/6$. The number 6 represents the ratio of the number of the tetrahedral sites to the number of the total metal atoms in the bcc unit cell. The function $J(\tau,\omega)$ is the spectral density for proton and vanadium, and is described by

$$J(\tau,\omega)=\frac{\alpha}{(1+\alpha)^2}\cdot\frac{\tau}{1+\omega^2\tau^2}\ . \tag{4}$$

In Eq. (4), $\alpha=\exp(\epsilon/RT)$, in which ϵ is the difference in the potential depth between the two sites. If the potential depth of the deeper potential well is given by E, the correlation time τ, for fluctuation of the nuclear spins, is represented by $\tau_0\exp(-E/RT)(1+\alpha)^{-1}$. In this system, the correlation time between protons is defined as τ and that between ^{1}H and ^{51}V spins can be regarded as 2τ, since the vanadium atom is fixed.

F_{VH} and F_{HH} are functions of interatomic distances and angles, which are determined only by geometry of the crystal structure if the two sites are defined. These quantities are the dipolar interactions reduced by the fluctuation of the dipolar vectors. When all the tetrahedral sites are fulfilled by hydrogen atoms, F_{VH} and F_{HH} for the powder sample are given by[28]

$$F_{\mathrm{VH}}=\sum_k R_{1k}^{-6}+\sum_l R_{2l}^{-6}-2\sum_{k,l}R_{1k}^{-3}R_{2l}^{-3}P_2(\cos\Omega_{Vkl})\ , \tag{5a}$$

$$F_{\mathrm{HH}}=\sum_k r_{1k}^{-6}+\sum_l r_{2l}^{-6}-2\sum_{k,l}r_{1k}^{-3}r_{2l}^{-3}P_2(\cos\Omega_{Hkl})\ , \tag{5b}$$

where R_{1k} and R_{2l} are vectors from a given V nucleus to the two hydrogen sites, k and l, between which the jump occurs, and r_{1k} and r_{2l} are vectors from a given proton to two other hydrogen sites k and l between which another proton jumps. $\Omega_{\mathrm{V}kl}$ and $\Omega_{\mathrm{H}kl}$ are the angle between those vectors. P_2 is the second Legendre polynomial. The summation is to be made over all the lattice points.

Next we expand the above formulas to Brouwer's local-structure model described in Fig. 3. If the jump of the hydrogen atom occurs between the sites shown in the figure, the total T_1^{-1} is described by the summation of contributions from the jump between i and j sites, selected out of the five sites with a probability P_{ij}.[31] The probability P_{ij} is given by the product of p_i and p_j, which are the probabilities of the i site, $\mathrm{H(Ti_{4-}{}_iV_{}}_i)$, and the j site, $\mathrm{H(Ti_{4-}{}_jV_{}}_j)$, among the five kinds of sites, respectively,

$$P_{ij}=p_i\cdot p_j\ . \tag{6}$$

p_i is given by the binomial distribution for the alloys $\mathrm{Ti_{1-}{}_yV_{}}_y\mathrm{H}_x$,[18]

$$p_i=\binom{4}{i}(1-y)^{4-i}y^i\quad(i=0,1,\ldots,4)\ . \tag{7}$$

Using P_{ij} the total spectral densities $J(\tau,\omega)$ are described as the summation of the individual spectral densities $J(\tau_{ij},\omega)$

$$J(\tau,\omega)=\sum_{i,j}P_{ij}\cdot J(\tau_{ij},\omega)\ , \tag{8}$$

where τ_{ij} represents the correlation time characterizing the jump rate between the i and j sites and given by

$$\tau_{ij}=\tau_0\exp(-E_i/RT)(1+\alpha_{ij})^{-1}\ ,$$

in which α_{ij} is the difference in the populations between the two sites, and τ_0 is a prefactor. $\alpha_{ij}=\exp(\epsilon_{ij}/RT)$, in which ϵ_{ij} is the unequality of the potential depth between the i and j sites, and is given by

$$\epsilon_{ij}=E_i-E_j\ . \tag{9}$$

The expression of Eq. (8) is exactly the same as the spectral density with distribution of the correlation times. In this treatment, the origin of the distribution is the existence of the five kinds of hydrogen sites in β-$\mathrm{Ti_{1-}{}_yV_{}}_y\mathrm{H}_x$.

We assume that the potential depth corresponding to the individual hydrogen site is proportional to the fraction of the vanadium, y. Then E_i is given by

$$E_i=\frac{(4-i)E_{\mathrm{Ti}}+iE_{\mathrm{V}}}{4} . \quad (10)$$

E_{Ti} and E_{V} are the activation energies for $H(Ti_4V_0)$ and $H(Ti_0V_4)$, respectively. In Eqs. (1)–(10), adjustable parameters are τ_0, E_{Ti}, and E_{V}. The two-site jump model combined with Brouwer's local-structure model, which is applied to the Ti-V-H system in this work, will be generally developed in other binary-alloy systems with high hydrogen content.

We will explain the experimental results using Eqs. (1)–(10), and discuss our model comparing with the simple isotropic diffusion model. For the contribution of the conduction electrons in Eq. (1), we assume that the K value in the Korringa relation for $Ti_{1-y}V_yH_x$ is given by the weighted average of the K's for TiH_x (Ref. 32) and VH_x (Ref. 33), as listed in Table II.

We also calculate the parameters F_{VH} and F_{HH} in Eqs. (5a) and (5b) on the basis of the crystal structures of the alloys under the following assumptions: (1) The distances between hydrogen atoms are larger than 0.21 nm.[34,35] In other words, hydrogen atoms do not simultaneously occupy the neighboring sites between which the distance is less than 0.21 nm. In β-Ti-V-H, the first-, the second-, and the third-nearest-neighbor sites from an occupied site are empty, as indicated in Table I. (2) We take account of the hydrogen jumps from a given site to up to its third-nearest-neighbor sites, all of which are empty. Hydrogen atoms can jump to an empty site. Long-distance jumps are neglected because of the low probability of the jumps and the presence of occupied sites. The number of sites of hydrogen for the first-, second-, and third-nearest neighbors are 4, 2, and 8, respectively, as shown in Fig. 4. (3) The probabilities of the hydrogen jump from the initial to the other sites are approximated to be equal for all the 14 sites for simplification, although the actual probability is expected to decay as a function of distance from the initial site. Consequently, in our model, the jump probability vs the distance is expressed by a square distribution function, which has a constant value from the first-nearest-neighbor site to the third and becomes zero at the fourth.

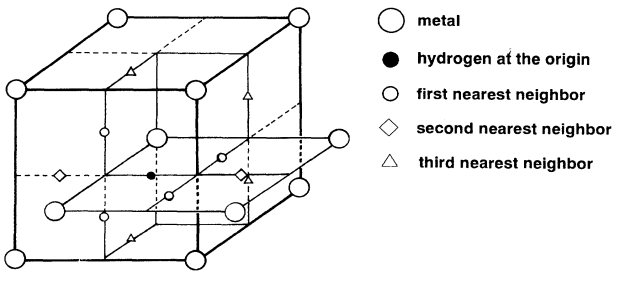

FIG. 4. A bcc unit cell and tetrahedral sites. A hydrogen atom jumps from an initial site (●) to one of the neighboring sites, which are four first-nearest neighbors (○), two second-nearest neighbors (◇), and eight third-nearest neighbors (△). The mark ○ indicates the metal atoms.

The full dipolar interactions determining the linewidth in rigid lattice can be calculated by $\sum r_{ij}^{-6}$ simple summation over all the tetrahedral sites except for the sites which are specified by the above assumption (1). The F_{VH} and F_{HH} values estimated in our model are $1443\times a_0^{-6}$ and $509.4\times a_0^{-6}$, respectively, where a_0 is the lattice constant of the bcc structure. These values are 55 and 39% of the full dipolar interactions, which means that 55 and 39% of the full dipolar interactions contribute to the relaxation. On the other hand, 75% of the full dipolar interactions contribute to the relaxation in the simple isotropic diffusion model where the above assumption (1) is valid also.[36]

The best agreement between the experimental and the calculated T_1 values is obtained for the following parameters: $\tau_0=1.5\times10^{-11}$ s, $E_{\mathrm{ti}}=16$ kJ/mol, and $E_{\mathrm{V}}=9.5$ kJ/mol, which are listed in Table II. The calculated T_1 values are shown by solid lines in Figs. 1 and 2. Although the number of the adjustable parameters is only three, the experimental T_1 values for $Ti_{0.2}V_{0.8}H_{0.83}$, $Ti_{0.4}V_{0.6}H_{0.91}$, and $Ti_{0.6}V_{0.4}H_{0.91}$ can be well fitted. The E_{Ti} and E_{V} obtained from the alloy hydrides in this work agree with those for $TiH_{0.70}$ and $V_{0.9}Cr_{0.1}H_{0.65}$, which are 14.2 (Ref. 32) and 9.7 kJ/mol (Ref. 37), respectively.

Our model has succeeded in solving the following three discrepancies encountered in the isotropic diffusion model: (1) the differences in the T_1 minimum values between the experimental and the calculated ones, and (2) the asymmetry of the T_1 vs $1/T$ plots. The fractions of the dipolar interactions contributing to T_1 are much smaller in our model than in the isotropic diffusion model. Consequently, the minimum values of T_1 calculated in our model are larger than those in the isotropic diffusion model. In addition, the distribution of τ_{ij} leads to the increase in the minimum values of T_1 and produces the asymmetry in the T_1 vs $1/T$ plots. (3) The radius of the curvature in the T_1 vs $1/T$ plot decreases with increase in the Ti concentrations. This trend can be explained completely by our model, but not by the isotropic diffusion model. In our model, the T_1 of proton is represented by a weighted mean of fractional T_1 values corresponding to the hydrogen jumps between a pair of sites as described in Eq. (8). The largest gradient and the smallest radius of the curvature in the fractional $T_1(\tau_{ij})$ vs $1/T$ plot are expected for the hydrogen jumps between sites having the deepest potential depth, $H(Ti_4V_0)$. Therefore, with increase in the fraction of Ti the T_1 vs $1/T$ plot shows the decrease in the radius of the curvature because of the increase in the fraction of the $H(Ti_4V_0)$ sites.

Although the calculated values show good agreement with the experimental data, slight discrepancies remain unsolved. First, the frequency dependence in the high-temperature range shown in Fig. 1 can be interpreted by neither our model nor the isotropic diffusion model. Both models predict that the T_1 values are independent of frequency. To solve this problem Sholl[38] has suggested that the hydrogen motion over the long-range distances might occur as if it were the diffusion in the liquid state.

On the basis of the fluid mechanical approximation, he showed that the spectral densities $J(\omega)$ are proportional to $\omega^{-1/2}$ in the high-temperature range. Therefore, the T_1 values should have the contribution proportional to the square-root of frequency, $\omega^{1/2}$. This frequency dependence has been observed experimentally by Salibi and Cotts.[39] Our model does not include the effect of the diffusion over the long-range distances to the extent of several lattices.

Second, systematic deviations are found between the calculated and experimental values in the lowest-temperature range about 105~150 K. For example, the experimental T_1 values for $Ti_{0.4}V_{0.6}H_{0.91}$ at 90 MHz are 255 and 250 ms at 143 and 121 K, respectively, whereas the calculated values are 402 and 613 ms. The experimental values tend to be smaller than the calculated ones, and the deviation becomes larger with decrease in the temperature. Three possible origins may explain this deviation: The first is that the contribution from the conduction electrons is much larger than what we have expected. The second is that there is a limitation of T_1 by proton cross relaxation to quadrupolar-broadened metal nuclides.[40] The third is the presence of another relaxation mode easily excited in the metals and alloys, such as phonon-assisted tunneling of the hydrogen atoms suggested by neutron inelastic scattering for VH_x,[41] NbH_x,[41–43] and ScH_x.[44] This mechanism may have a little contribution to the relaxation in the temperature range between 110 and 140 K. Further studies such as ^2H NMR measurements should be carried out to make these points clearer.

In our model, the calculated T_1 values agree fairly well with experimental ones irrespective of the simple approximations. It is possible to improve the agreements with further precise approximations.

[1] *Constitution of Binary Alloys,* 2nd ed., edited by M. Hansen (McGraw-Hill, New York, 1958), p. 1241.
[2] H. Nagel and R. S. Perkins, Z. Metallkd. **66**, 362 (1975).
[3] S. Ono, K. Nomura, and Y. Ikeda, J. Less-Common Met. **72**, 159 (1983).
[4] S. Hayashi, K. Hayamizu, and O. Yamamoto, J. Less-Common Met. **113**, 1 (1985).
[5] R. C. Bowman, Jr. and W.-K. Rhim, Phys. Rev. B **24**, 2232 (1981).
[6] B. Nowak and M. Minier, J. Less-Common Met. **101**, 245 (1984).
[7] B. Nowak, Y. Chabre, and R. Andreani, J. Less-Common Met. **130**, 193 (1987).
[8] B. Nowak, S. Hayashi, K. Hayamizu, and O. Yamamoto, J. Less-Common Met. **123**, 75 (1986).
[9] S. Hayashi, K. Hayamizu, and O. Yamamoto, J. Solid-State Chem. **46**, 306 (1983).
[10] S. Hayashi, K. Hayamizu, and O. Yamamoto, J. Chem. Phys. **78**, 5096 (1983).
[11] S. Hayashi and K. Hayamizu, J. Less-Common Met. **161**, 61 (1990).
[12] T. Ueda, S. Hayashi, and K. Hayamizu (unpublished).
[13] N. Bloembergen, E. M. Purcell, and R. V. Pound, Phys. Rev. **73**, 679 (1948).
[14] J. Hauck and H. J. Schenk, J. Less-Common Met. **51**, 251 (1977).
[15] C. Korn, Phys. Rev. B **17**, 1707 (1978).
[16] S. Kazama and Y. Fukai, J. Phys. Soc. Jpn. **42**, 119 (1977).
[17] R. C. Brouwer, E. Salomons, and R. Griessen, Phys. Rev. B **38**, 10 217 (1988).
[18] R. C. Brouwer, J. Rector, N. Koeman, and R. Griessen, Phys. Rev. B **40**, 3546 (1989).
[19] R. A. Oriani, Acta Metall. **18**, 147 (1970).
[20] M. Koiwa, Acta Metall. **22**, 1259 (1974).
[21] R. Kirchheim, Acta Metall. **30**, 1069 (1982).
[22] R. Griessen, Phys. Rev. B **27**, 7575 (1983).
[23] H. D. Carstanjen and R. Sizmann, Ber. Bunsenges. Phys. Chem. **76**, 1223 (1972).
[24] M. Antonini and H. D. Carstanjen, Phys. Status Solidi A **34**, K153 (1976).
[25] V. A. Somenkov, I. R. Entin, A. Y. Chervayakov, S. Sh. Shil'stein, and A. A. Chertkov, Fiz. Tverd. Tela (Leningrad) **13**, 2587 (1971) [Sov. Phys. Solid State **13**, 2178 (1972)].
[26] D. C. Look and I. J. Lowe, J. Chem. Phys. **44**, 3437 (1966).
[27] J. E. Anderson, J. Magn. Reson **11**, 398 (1973).
[28] S. Takeda, G. Soda, and H. Chihara, Mol. Phys. **47**, 501 (1982).
[29] N. Imaoka, S. Takeda, and H. Chihara, Bull. Chem. Soc. Jpn. **61**, 1865 (1988).
[30] S. Takeda, H. Chihara, T. Inabe, T. Mitani, and Y. Maruyama, Chem. Phys. Lett. **189**, 13 (1992).
[31] P. A. Beckmann, Phys. Rep. **171**, 85 (1988).
[32] E. H. Sevilla and R. M. Cotts, Phys. Rev. B **37**, 6813 (1988).
[33] Y. Fukai and S. Kazama, Acta Metall. **25**, 59 (1977).
[34] A. C. Switendick, Z. Phys. Chem. Neue Folge **117**, 89 (1979).
[35] B. K. Rao and P. Jena, Phys. Rev. B **31**, 6726 (1985).
[36] A. Abragam, *Principles of Nuclear Magnetism* (Oxford University, New York, 1961), p. 111.
[37] D. Rohy and R. M. Cotts, Phys. Rev. B **1**, 2070 (1970).
[38] C. A. Sholl, J. Phys. C **14**, 447 (1981).
[39] N. Salibi and R. M. Cotts, Phys. Rev. B **27**, 2625 (1983).
[40] L. R. Lichty, J.-W. Han, D. R. Torgeson, R. G. Barnes, and E. F. W. Seymour, Phys. Rev. B **42**, 7734 (1990).
[41] I. Svare, Physica **145B**, 281 (1987).
[42] H. Wipf, K. Neumaier, A. Magerl, A. Heidemann, and W. Stirling, J. Less-Common. Met. **101**, 317 (1984).
[43] H. Wipf, D. Steinbinder, K. Neumaier, P. Gutsmiedl, A. Magerl, and A. J. Dianoux, Europhys. Lett. **4**, 1379 (1987).
[44] T. J. Udovic, J. J. Rush, I. S. Anderson, and R. G. Barnes, Phys. Rev. B **41**, 3460 (1990).